Digest Journal of Nanomaterials and Biostructures Vol. 6, No 3, July- September 2011, p. 943 - 951

SYNTHESIS OF ROD-LIKE MAGNETITE BY USING LOW MAGNETIC FIELD

D. FICAI*, A. FICAI, B. S. VASILE, M. FICAI, O. OPREA, C. GURAN, E. ANDRONESCU
POLITEHNICA University of Bucharest, Faculty of Applied Chemistry and Material Science; 1-7 Polizu Str., 011061 Bucharest, Romania

Magnetic (nano)particles are intensively studied in the last years due to their multiple applications. The purpose of this paper is the synthesis of rod-like magnetite by magnetically assisted co-precipitation. The synthesized magnetite nanoparticles were characterized by XRD, DSC-TG and TEM from compositional and especially morphological point of view. The use of 0.5T magnetic field induces a preferential growth of magnetite nanoparticles on the 400 direction while this preferential growth cannot be identified in the absence of the magnetic field proving that the synthesis of rod-like magnetite is due to the applied magnetic field. The mechanism of synthesis was explained based on the magnetite particles behaviour in magnetic field.

(Received March 7, 2011 Accepted May 14, 2011)

Keywords: rod-like magnetite; magnetic field; assisted co-precipitation; TEM

1. Introduction

Due to the potential application of the magnetic nanoparticles, these materials were extensively studied. Special attention was paid for the synthesis of different $Me^{2+}Fe_2O_4$ under different precipitation conditions [1-4]. Most known synthesis methods of the magnetite nanoparticles are: coprecipitation methods [5], hydrothermal reaction [6], sonochemical decomposition of hydrolyzed Fe^{2+} salt [7] or γ-iradiation of β-FeOOH [8].

Magnetite is widely used for medical and non-medical applications. The main medical applications can be divided in both diagnosis (magnetic contrast agent) and therapy (drug delivery, drug carrier and hyperthermia) [9]. Magnetite properties are strongly influenced by the composition and morphology of magnetite.

Magnetite particles are synthesized both in vitro and in vivo (for instance in bacteria). It is worth to mention that magnetite crystals synthesized by bacteria have high chemical purity, well-defined morphologies, narrow size and shape distribution and, many times, unusual shapes [10, 11].

From the morphological point of view researcher tried to synthesize size-controlled magnetic nanoparticles with smaller and smaller particles size [2, 7, 12] but only in a few articles the synthesis of shape-controlled magnetic nanoparticles were presented [13-15].

Recently, the fabrication of shape controlled magnetite nanostructure was published by Zheng et al. [16]. They concluded that magnetite shape can be controlled by precursor's concentrations and molecular weight of the polyethylene glycol which is used as dispersant. They found that cubic magnetite is obtained if 0.2M Fe^{3+}, 0.1M Fe^{2+} and 10^{-3}mol/L PEG (M.W.=20.000) solutions are used; nanorods with geometrical characteristics of 10nm x 100-200nm are obtained if solutions of $2.0x10^{-2}$ Fe^{3+}, $1.0x10^{-2}$ Fe^{2+} and 10^{-3}mol/L PEG (M.W.=20.000) are used and dendrides are obtained if solutions of $2.0x10^{-3}$ Fe^{3+}, $1.0x10^{-3}$ Fe^{2+} and $2.0x10^{-3}$mol/L PEG (M.W.=20.000) are used. Also, the molecular weight of PEG leads to morphological changes of

*Corresponding author: manzu_denisa76@yahoo.com

the magnetite nanostructures. Thereby, spherical magnetite nanoparticles with an average diameter of 15nm were obtained when PEG 400 was used; nanorods having 20nm diameter and about 150nm long when PEG 10.000 was used and nanowires of some hundreds nanometers when PEG 100.000 was used, in all cases the precursors concentrations were $2.0x10^{-2}$ Fe^{3+}, $1.0x10^{-2}$ Fe^{2+} and 10^{-3} mol/L PEG.

In this paper we present the synthesis of rod-like magnetite. The synthesis of rod-like magnetite is an essential step for obtaining improved magnetic materials with potential application in hyperthermia. The main advantage of the rod-like magnetite is the improved mobility of this kind of particles reporting to the spherical one with same weight.

2. Experimental

2.1. Materials

Magnetite was synthesized starting from $FeCl_2 \cdot 4H_2O$ and $FeCl_3 \cdot 6H_2O$ as precursors (p.a., Merck) by precipitation with 20% NaOH (Sigma Aldrich, p.a.) solution.

2.2. Equipment

The resulting particles were investigated by X-ray diffraction (XRD), thermal analysis (DTA-TGA), scanning electron microscopy (SEM) and transmission electron microscopy (TEM).

X-ray diffraction analysis was performed using a Shimadzu XRD 6000 diffractometer at room temperature, using Cu Kα radiation. The samples were scanned in the Bragg angle, 2θ range of 10 – 70, with a scanning rate of 2^0/min.

The thermal analysis of the magnetite was followed with a Netzsch TG 449C STA Jupiter instrument. Samples were screened to 200 mesh prior to analysis then was placed in alumina crucible and heated with $10K \cdot min^{-1}$ from room temperature to 800 ^oC, under the flow of 20 mL min^{-1} dried synthetic air (80% N_2 and 20% O_2).

Scanning electron microscopy images were obtained with a HITACHI S2600N microscope coupled with an EDS probe. All samples were covered with a silver layer prior to imaging.

The transmission electron images were obtained on finely powdered samples using a Tecnai^{TM} G^2 F30 S-TWIN high resolution transmission electron microscope (HRTEM) from FEI. The microscope was operated in transmission mode at 300kV with TEM point resolution of 2 Å and line resolution of 1 Å. The finely MNPs powder was dispersed into pure ethanol and ultrasonicated for 15 minutes. After that one small drop of the diluted sample was put onto a holey carbon coated copper grid and left to dry before it was analyzed through TEM.

2.3. Synthesis method

The magnetite particles were obtained by co-precipitation from aqueous solution by starting from $FeCl_2$ and $FeCl_3$ as precursors (both purchased from Merk) at strongly basic pH (pH=12, the pH was realized by drop wise addition of 20% NaOH solution), at 25°C. The molar ratio between the precursors was Fe^{2+}:Fe^{3+} = 1:2 (Fe^{3+}=0.5M and Fe^{2+}=0.25M).

The synthesis of rod-like magnetite is induced by the applying of 0.5T magnetic field during the co precipitation step. The magnetic field is realized by placing a permanent magnet at the bottom of the synthesis flask. The mechanism of the synthesis of the rod-like magnetite can be illustrated based on the influence of the magnetic field on the magnetite particle. At macroscopic scale, it can be seen that magnetite powder is associated into rods-like structures when magnetic field is applied, the rods being oriented along the magnetic field pattern Figure 1a. The mechanism of rod-like magnetite synthesis in magnetic field can be easily explained based on the above observations and the synthesis route. Therefore, along with the NaOH addition, the pH increases and induces MNPs formation (usually as very small crystals).

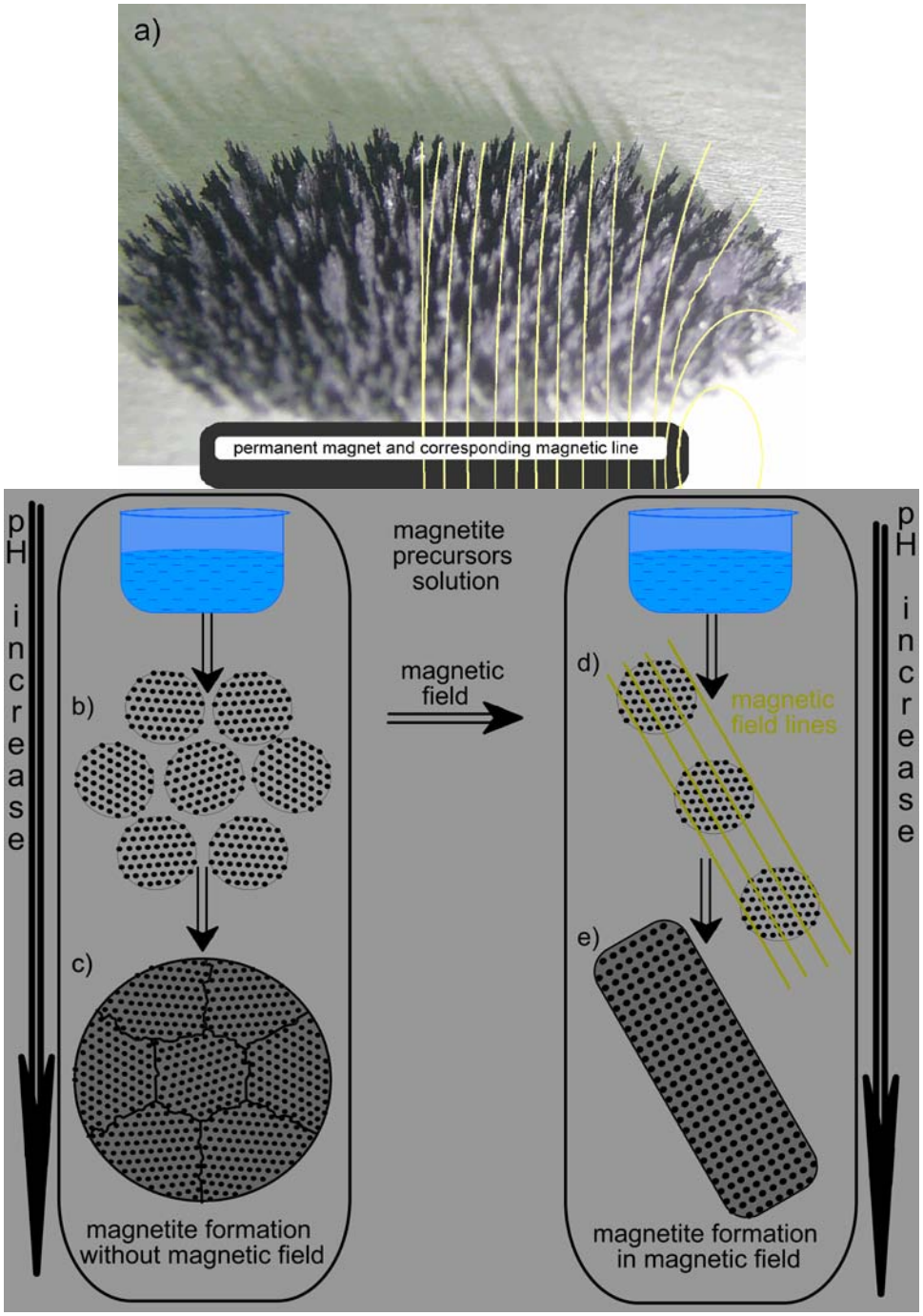

Fig. 1. Magnetic field behavior of magnetite powder

If no magnetic field is present spherical nanocrystals are formed. It has to mention that, the assembling of these nanocrystals is controlled by the own magnetic moment of these nanocrystals which leads to spherical or quasispherical particles as we represented in Figure 1c.

When magnetic field is applied, the nanocrystals became arranged alongside magnetic field lines. With the increase of the pH, the amount of magnetite increase and nanorods-like magnetite particles are formed Figure 1e.

The formation of the rod-like particle is possible if magnetic field is applied during the precipitation of the magnetite, the condition is to apply the magnetic field before the structures presented in Figure 1c are formed. It has to mention that starting from the initial magnetite nucleation centres (Figure 1b), magnetite nanoparticles growth during the precipitation process, the presence of the magnetic field assuring the special morphology of these nanoparticles.

Whatever of the used synthesis method (in the presence or in the absence of magnetic field), the magnetite precipitate was washed with plenty of water until pH=7 followed by the freeze drying of the precipitate. The freeze drying method was used in order to limit the agglomeration of the nanoparticles.

2.4. Fe^{2+}:Fe^{3+} molar ratio determination

The Fe^{2+}:Fe^{3+} molar ratio was determined after individual determination of Fe^{2+} and Fe^{3+}. In the first step, magnetite is dissolved in 3M H_2SO_4, diluted with distilled water and titrate with $Ce(SO_4)_2$. The potentiometric redox titration allows the quantitative determination of Fe^{2+} based on the equivalence point determined by monitoring the electromotive force of the electrochemical cell (Pt working electrode and Ag/AgCl reference electrode) by using a PCD6500 multiparameter. In the second step, the total content of Fe^{3+} is spectrophotometrically determined at 460cm^{-1} and pH=5.2 (acetate buffer). The absorbance – concentration correlation is made based on the obtained calibration curve. For calibration, 5 standard samples (in the range of 0.01-1mM) were obtained and measured using the UV-Vis spectrometer (Thermo Evolution 300) and plotted the absorbance versus concentration. All the standards were obtained starting from the corresponding amount of $FeCl_3$, 5mL acetate buffer 1M in 50 mL measuring flask. The absorbance of all the standards, as well as the sample was measured at 460cm^{-1} versus blank solution (the blank solution is obtained in the same way as the standard solutions but doesn't contain Fe^{3+}).

3. Results and discussion

3.1. Elemental analysis

The Fe^{2+}:Fe^{3+} molar ratio was determined in order to distinguish Fe_3O_4 from Fe_2O_3, oxides which can't be discerned only by XRD. The Fe^{2+}:Fe^{3+} molar ratio was determined as presented in section 2.4 and proves that the obtained magnetite is highly pure (the experimental Fe^{2+}:Fe^{3+} ratio being 1.51 while the theoretical molar ratio is 1.5).

3.2. X-ray diffraction

XRD pattern of the rod-like magnetite obtained in magnetic field has some particularities versus the reference magnetite sample. The main difference between the two samples is the relative intensities of the characteristic peaks.

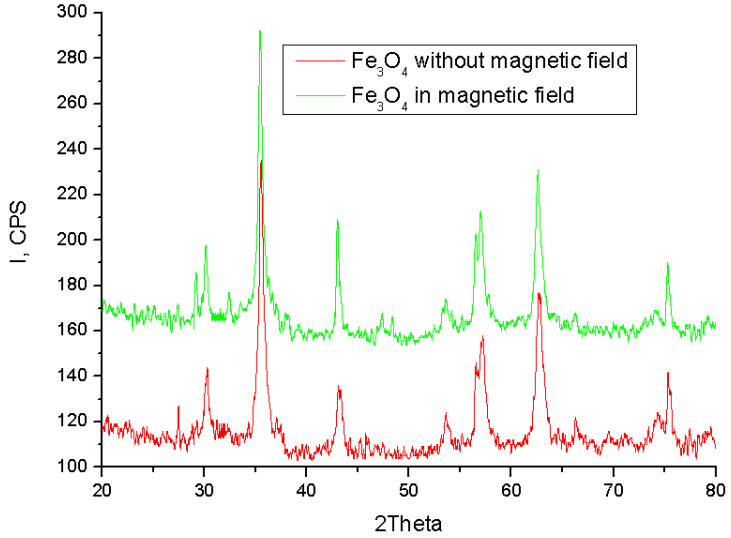

Fig. 2. XRD patterns of MNPs obtained with and without 0.5T magnetic field

The presence of the 0.5T magnetic field induces a preferential growth on the 400 direction. Analysing the main characteristic peaks corresponding to magnetite it can seen that the use of 0.5T magnetic field leads to a decrease of the intensity of the peaks corresponding to 422; the ratio of the relative intensity corresponding to this direction is ~1.68. Reporting the crystallite size of the two synthesized MNPs (under 0.5T magnetic field and without magnetic field) it can be seen that only the size of the crystallite growth on the 220, 400, 333, 440 directions are influenced while the crystallite growth on 311, 422, 533 practically are not influenced by the applied 0.5T magnetic field. Among the crystallites only the MNPs growth on the 400 direction increase as size while the others, growth on 220, 333 and 440, remain the same or even decrease.

Table 1. Main crystallographic characteristics of MNPs obtained with and without 0.5T magnetic field

2θ	**hkl**	**d(Å)**	**D_{hkl} crystallite size of MNPs obtained**		**Relative peaks intensity (%)**	**Crystallite size ratio 5:4**
			without	**with 0.5T**		
			magnetic field (nm)			
1	**2**	**3**	**4**	**5**	**6**	**7**
30.3	220	2.968	44	26	1.12	0.59
35.5	311	2.535	20	19	1	0.95
43.1	400	2.09	23	33	1.68	1.43
53.5	422	1.719	38	38	0.88	1.00
57.2	333	1.614	45	23	1.03	0.51
62.5	440	1.478	34	20	0.96	0.59
75.3	533	1.271	41	43	0.95	1.05

3.3. TEM

TEM bright images were recorded in order to characterize the MNPs from the point of view of particles' size and shape. In the absence of the magnetic field (Figure 3a), spherical MNPs nanoparticles were obtained with an average particles size of ~7nm. By applying a 0.5T magnetic field almost all of the MNPs became rod-like. Also it can be seen that some nanoparticles remained spherical but the amount being relative reduced. The size of rod-like MNPs have D*h=(7-20nm)*(20-60 nm).

The inset shown in figure 4b represents the selected area diffraction pattern, obtained on MNPs nanopowder which was synthesised in the presence of magnetic field, from which we can state that the only phase identified is of cubic form of Fe_3O_4.

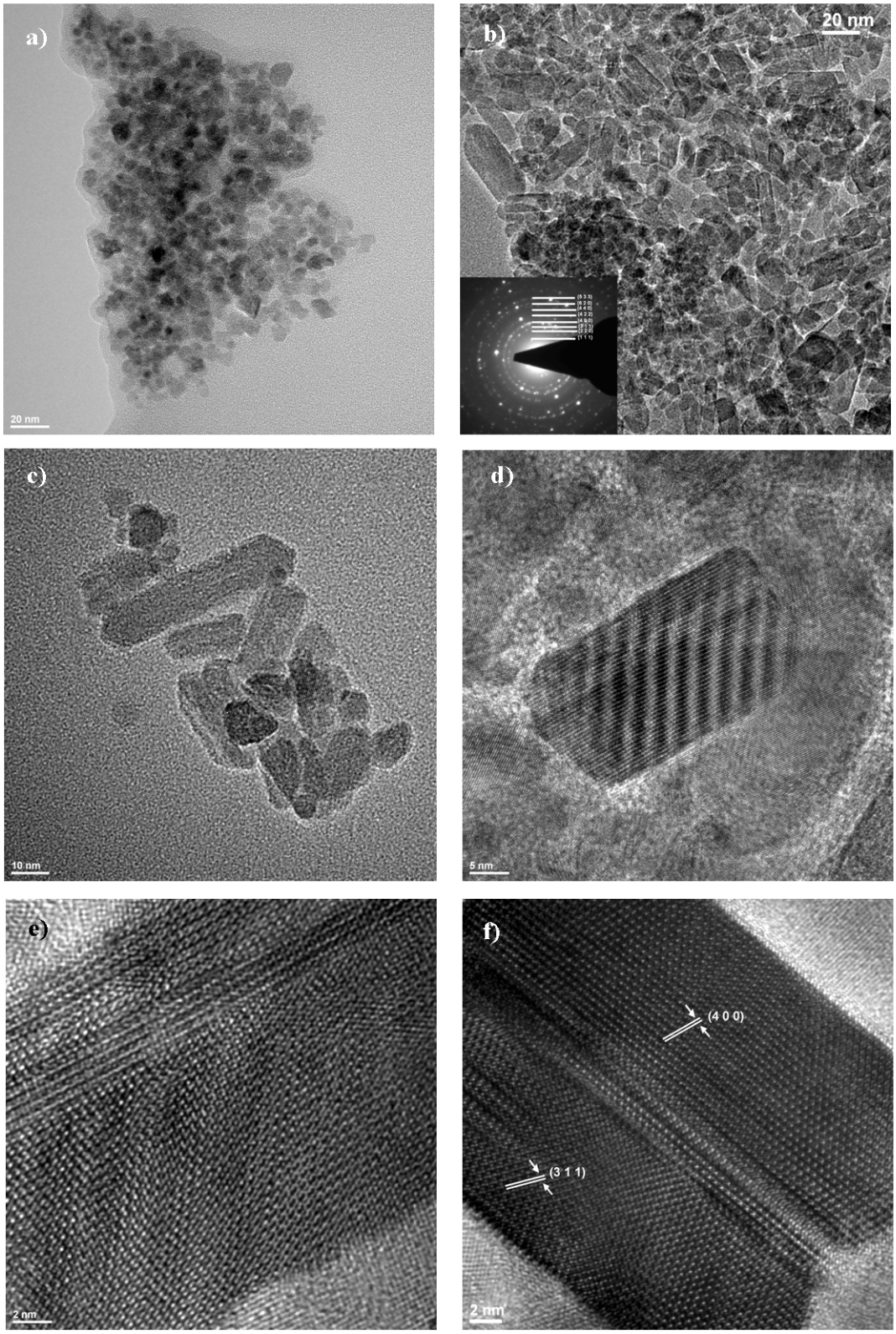

Figure 3. TEM bright field and HRTEM images of magnetite nanoparticles synthesized: a) without magnetic field; b-f) under 0.5T magnetic field, at different magnification

HRTEM images obtained on MNPs nanoparticles (fig. 4 e,f), with magnetic field applied, shows clear lattice fringes of d=2.53Å and d=2.09Å corresponding to 311 and 400 crystallographic planes of cubic Fe_3O_4.

It can be stated that the presence of 0.5T magnetic field induces a special rod-like morphology of MNPs.

3.4. Thermal analysis

Magnetite, Fe_3O_4, is metastable in air below about 1000°C compared to the fully oxidized hematite, α-Fe_2O_3 [17]. Consequently, the existence of magnetite at lower temperatures is dependent on its kinetic stability. The reactivity of magnetite therefore depends on many factors, e.g., surface area, impurities, defects, etc [18]. Magnetite prepared at relatively low temperatures from freshly precipitated precursors has a much greater surface area and defect concentration and therefore oxidizes at lower temperatures [19]. The process of magnetite oxidation has been shown to go through the intermediate product, metastable γ-Fe_2O_3 [18].

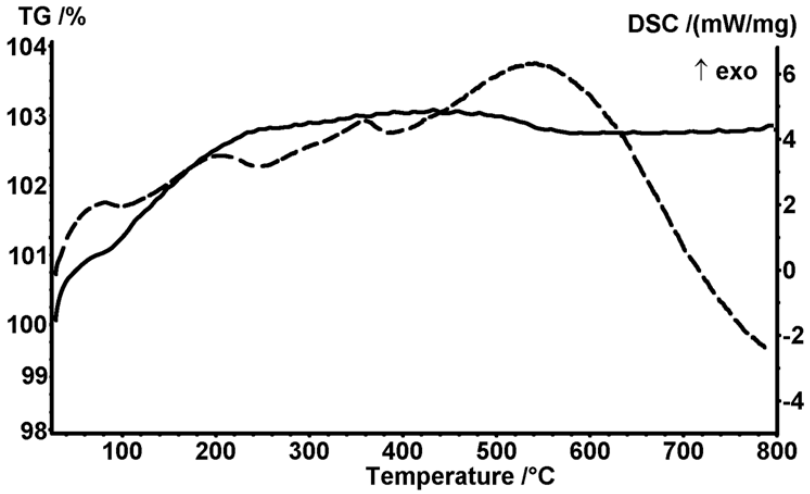

Fig. 4. The TG-DSC for magnetite synthesized without magnetic field

Thermal analysis of the magnetite sample synthesized without magnetic field is presented in Figure 4. The process of oxidation involves two stages. First stage, up to 120°C, with an experimental mass gain of 1.05% can be attributed to Fe(II) oxidation due to water molecules and OH moieties that were trapped inside the sample during synthesis phase [20]. This stage has associated an exothermic effect on DSC curve.

After 120°C the sample's mass continuously increase slowly until 240°C, the experimental mass gain being an additional 1.70%. This process has associated also an exothermic effect. This stage was attributed to the surface oxidation of the Fe(II) with formation of maghemite phase (γ-Fe_2O_3) [18]. A further DSC exothermic peak at 355°C was attributed to oxygen diffusion in the core of the particles and complete transformation to γ-Fe_2O_3.

The broad exothermic effect at 550°C was attributed to phase transition from γ-Fe_2O_3 to α-Fe_2O_3 (maghemite to hematite transition). The total mass change is 2.91% (well below to the theoretical value of 3.46 mass%). The difference was assigned to the water molecules and OH moieties trapped during synthesis, which contributes to oxidation of Fe(II) but do not add to the mass.

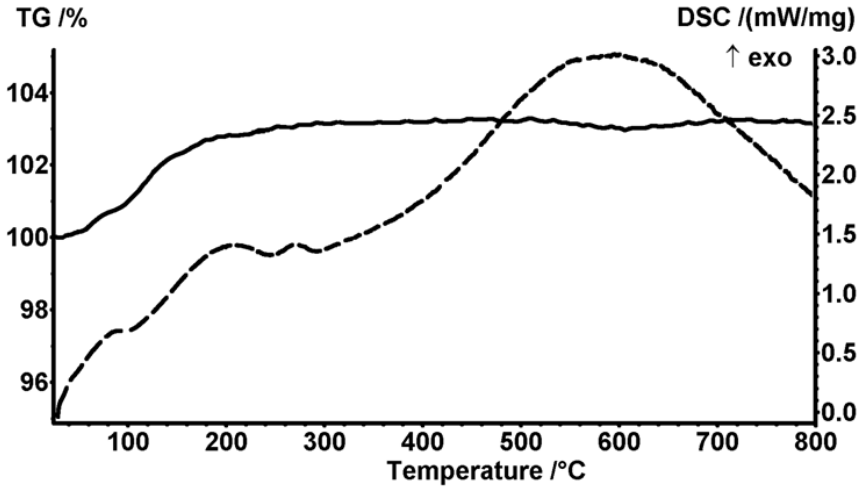

Fig. 5. The TG-DSC for magnetite synthesized with magnetic field

Thermal analysis of the magnetite sample synthesized with magnetic field is presented in Fig. 5. The sample exhibits a similar pattern of oxidation up to 220^{o}C, with a mass gain of 2.95%. The DSC exothermic effect attributed to oxygen diffusion in the core of the particles and complete oxidation to γ-Fe_2O_3 appears at 270^{o}C (vs. 355^{o}C in the magnetite synthesized without magnetic field) and has a lower intensity. The rod shape of the magnetite obtained with magnetic field can explain this shift to lower temperature of the core oxidation process, and the lower intensity of the effect seen on DSC curve.

The DSC broad peak corresponding to maghemite-hematite phase transition appears at 590^{o}C.

The total mass gain is 3.14%, higher than in the case of magnetite synthesized without magnetic field, pointing to a smaller percentage of trapped water molecules or –OH moieties, which is also in agreement with the rod shape of this magnetite.

4. Conclusion

In this paper the synthesis of rod-like magnetite by the use of low magnetic field of 0.5T as well as the proposed mechanism is presented. The preferential growth of magnetite can be clearly evidentiated by TEM and XRD.

By TEM it can seen that the use of 0.5T magnetic field leads to rod-like magnetite with the size of rod-like MNPs of D*h=(7-20nm)*(20-60nm).

By XRD it can be identify the most important peaks of the magnetite. The relative intensity of these peaks being changed when 0.5T magnetic field is applied comparing with the case of magnetite co-precipitation without magnetic field. Based on the relative intensity, it can conclude that the application of 0.5T magnetic field induce a preferential growth on the 400 direction. Same result is obtained comparing the size of crystallites determined based on Sherer formula, the crystallite corresponding to 400 increasing from 23nm to 33nm while the other crystallite decrease more or less.

Aknowledgements

Authors recognize financial support from the European Social Fund through POSDRU/89/1.5/S/54785 project: "Postdoctoral Program for Advanced Research in the field of nanomaterials”.

Reference

[1] Â. L. Andrade, D. M. Souza, M. C. Pereira, J. D. Fabris, R. Z. Domingues, Quim. Nova **33,** 524 (2010).
[2] P. Sipos, Romanian Reports in Physics **58**, 269 (2006).
[3] J. R. Correa, D. Canetti, R. Castillo, J. C. Llópiz, J. Dufour, Materials Research Bulletin **41,** 703 (2006).
[4] R. Massart, IEEE Transactions on Magnetics **2**, 1247 (1981).
[5] S. Si, C. Li, X. Wang, D. Yu, Q. Peng, Y. Li, Crystal Growth & Design **5**, 391 (2005).
[6] T. Fried, G. Shemer, G. Markovich, Advanced Materials **13**, 1158 (2001).
[7] S. Sun, H. Zeng, Journal of American chemical Society **124**, 8204 (2002).
[8] S. Wang, H. Xin, Radiation Physics and Chemistry **56**, 567 (1999).
[9] E. Andronescu, M. Ficai, G. Voicu, D. Ficai, M. Maganu, A. Ficai, Journal of Materials Science - Materials in Medicine **21**, 2237 (2010).
[10] B. Arato, Z. Szanyi, C. Flies, D. Schuler, R. B. Frankel, P. R. Buseck, M. Posfai, American Mineralogist **90**, 123 (2005).
[11] J. L. Kirschvink, S.-B. R. Chang, Geology **12**, 559 (1984).
[12] S. Si, A. Kotal, T. K. Mandal, S. Giri, H. Nakamura, T. Kohara, Chem. Mater. **16.** 3489 (2004) -3496.
[13] I. Nyiro-Kósa, D. C. Nagy, M. Pósfai, European Journal of Mineralogy **21**, 293 (2009).
[14] S. Li, G. W. Qin, W. Pei, Y. Ren, Y. Zhang, C. Esling, L. Zuo, Journal of the American Ceramic Society **92**, 631 (2009).
[15] F. Vereda, J. de Vicente, R. Hidalgo-Alvarez, Colloids and Surfaces a-Physicochemical and Engineering Aspects **319**, 122 (2008).
[16] Y. Y. Zheng, X. B. Wang, L. Shang, C. R. Li, C. Cui, W. J. Dong, W. H. Tang, B. Y. Chen, Materials Characterization **61**, 489 (2010).
[17] H. E. McGannon, The Making, Shaping and Treating of Steel, in: United States Steel Corporation Pittsburgh, PA 1970.
[18] J. P. Sanders, P. K. Gallagher, Journal of Thermal Analysis and Calorimetry **72**, 777 (2003).
[19] E. I. Buzás (Ed.) Heyden Son, London 1974, p. 751.
[20] A. K. Galwey, M. E. Brown, Thermal decomposition of ionic solids, Elsevier, 1999.